

## Electric-field gradient at the Fe nucleus in $\epsilon$ -FeSi

M. Fanciulli, A. Zenkevich,\* I. Wenneker,† A. Svane, N. E. Christensen, and G. Weyer  
*Institute of Physics and Astronomy, University of Aarhus, DK-8000 Aarhus C, Denmark*  
 (Received 11 July 1996)

The sign of the electric-field gradient tensor component along the principal axis,  $V_{zz}$ , in  $\epsilon$ -FeSi has been determined by conversion electron Mössbauer spectroscopy measurements in an external magnetic field. Additional and independent determination of the  $V_{zz}$  sign has been provided by the asymmetry of the quadrupole doublet observed in polycrystalline samples and attributed to internal stress. The experimental results are corroborated by *ab initio* full potential linear muffin-tin orbital calculations. [S0163-1829(96)03446-7]

### I. INTRODUCTION

The renewed interest in  $\epsilon$ -FeSi, a nonmagnetic narrow-gap semiconductor,<sup>1,2</sup> is related to some unusual properties common to the class of Kondo insulators.<sup>3,4</sup>

The bulk stable iron-monosilicide has a simple cubic Bravais lattice with four Fe atoms and four Si atoms in a unit cell with coordinates  $(u, u, u)$ ,  $(\frac{1}{2} + u, \frac{1}{2} - u, \bar{u})$ ,  $(\bar{u}, \frac{1}{2} + u, \frac{1}{2} - u)$ ,  $(\frac{1}{2} - u, \bar{u}, \frac{1}{2} + u)$  where  $u_{\text{Fe}} = 0.1358$ ,  $u_{\text{Si}} = 0.844$ , and the lattice parameter  $a = 0.4493$  nm.<sup>5,6</sup> The space-group symmetry is  $P2_13(T^4)$ . The Fe local symmetry is trigonal, with only one Si nearest neighbor at 0.229 nm, three Si second neighbors at 0.236 nm and three Si third neighbors at 0.253 nm. The directions of the trigonal axes for the four Fe atoms are  $[\bar{1}\bar{1}\bar{1}]$ ,  $[\bar{1}11]$ ,  $[1\bar{1}1]$ ,  $[11\bar{1}]$  as shown in Fig. 1.

The observed unusual temperature dependence of the nuclear quadrupole interaction of the  $I = 3/2$  excited state of  $^{57}\text{Fe}$ , the magnetic susceptibility and the shift of the  $^{29}\text{Si}$  nuclear magnetic resonance have been attributed to thermal activation of electrons across a narrow energy gap of about 0.05 eV.<sup>1</sup> Other models of these phenomena involve strong magnetic fluctuations.<sup>7-10</sup>

While the temperature dependence of the quadrupole interaction has been investigated the complete characterization of the electric-field gradient (EFG) at the Fe site in  $\epsilon$ -FeSi is still missing the experimental determination of the sign of the EFG component along the principal axis ( $V_{zz}$ ). The sign of  $V_{zz}$  in  $\epsilon$ -FeSi represents also important information to be compared with recent theoretical calculations of the EFG in different iron compounds.<sup>11,12</sup> Due to the particular crystal structure, as discussed in Sec. III, the sign of  $V_{zz}$  cannot be determined by measuring the angular dependence of the line intensities of the quadrupole doublet. A different approach, proposed by Ruby and Flinn,<sup>13</sup> is based on a magnetic perturbation technique.

The very good statistical accuracy and high resolution of the present conversion electron Mössbauer spectroscopy (CEMS) investigation allowed the determination of the sign of  $V_{zz}$  and the understanding of the peculiar asymmetry observed in polycrystalline samples grown on Si. The latter effect, related to stress, provides an additional independent determination of the sign of  $V_{zz}$ .

These results are compared with *ab initio* full potential

linear muffin-tin orbital (LMTO) calculations within the local density approximation of the EFG parameters.

### II. EXPERIMENTAL METHODS

$\epsilon$ -FeSi samples were produced by annealing an  $^{57}\text{Fe}$  (95.5% enriched) layer grown on Si(111) substrates by pulsed laser deposition at room temperature in a UHV chamber with a base pressure of  $5 \times 10^{-8}$  Pa. The thermal treatment at 380 °C in a vacuum of  $10^{-4}$  Pa for 1 h results in the Si diffusion assisted formation of a 100 nm polycrystalline  $\epsilon$ -FeSi.<sup>14,15</sup> The samples (60 nm thick) used to determine the stress were grown on Si(111) stripes  $2 \times 15$  mm in size. The samples have been characterized by Rutherford backscattering (RBS) and x-ray diffraction (XRD) and found to be polycrystalline. CEMS measurements have been performed at room temperature using a 50 mCi  $^{57}\text{Co}$  in a Rh matrix source which was moved by a standard constant-acceleration drive. The samples were incorporated as electrodes in a parallel

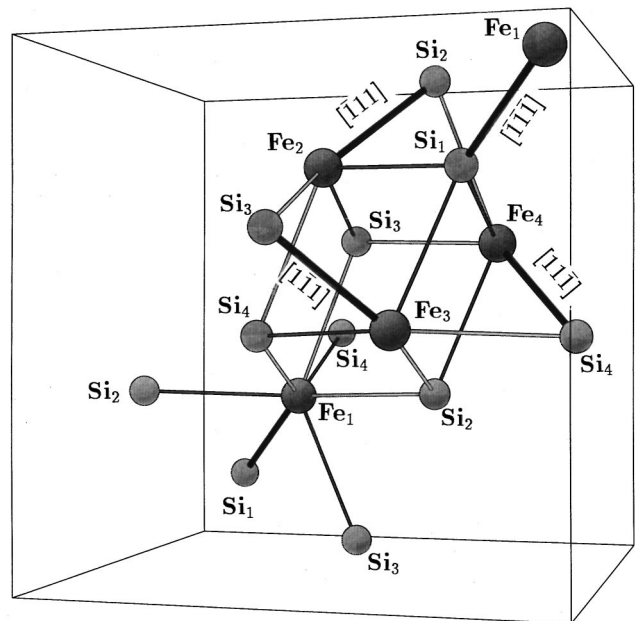


FIG. 1. The  $\epsilon$ -FeSi structure. The numbers 1, 2, 3, and 4 denote the atoms at positions  $(u, u, u)$ ,  $(\frac{1}{2} + u, \frac{1}{2} - u, \bar{u})$ ,  $(\bar{u}, \frac{1}{2} + u, \frac{1}{2} - u)$ ,  $(\frac{1}{2} - u, \bar{u}, \frac{1}{2} + u)$ , respectively.

plate avalanche detector.<sup>16</sup> The isomer shifts are given relative to  $\alpha$ -Fe. CEMS measurements in an external magnetic field up to  $H=1.3$  T have been carried out using a Varian magnet. The angle  $\alpha$  between the magnetic field  $H$  and the direction of emission of the  $\gamma$  quantum was  $\pi/2$ . Care has been taken to avoid significant broadening of the source linewidth due to the magnetic field. Calibration spectra using a  $^{57}\text{Fe}$  foil showed a linewidth of 0.238(1) mm/s with  $H=0$  and 0.258(2) mm/s with  $H=1.3$  T.

The stress has been determined by measuring the curvature of the Si stripes before and after silicide formation.

### III. EXPERIMENTAL RESULTS AND DISCUSSION

For a single-crystalline sample, the ratio of the intensity of the two transitions  $I_{1/2 \rightarrow 3/2}$  ( $I_\pi$ ) and  $I_{1/2 \rightarrow 1/2}$  ( $I_\sigma$ ) of a quadrupole doublet is angular dependent. If the asymmetry parameter  $\eta$  is zero and the Lamb-Mössbauer factor is isotropic one has<sup>17</sup>

$$\frac{I_\pi}{I_\sigma} = \frac{3(1 + \cos^2\Theta)}{5 - 3\cos^2\Theta}, \quad (1)$$

where  $\Theta$  is the angle between the direction of emission of the  $\gamma$  quantum and the principal axis of the EFG tensor. This angular dependence can be utilized to determine the sign of the EFG component along the principal axis. For example, it has been successfully used to characterize the EFG at the two iron sites in  $\beta$ -FeSi<sub>2</sub>.<sup>18,19</sup> However, in the case of  $\epsilon$ -FeSi the ratio of the intensity of the two transitions is, according to Eq. (1)

$$\frac{I_\pi}{I_\sigma} = \frac{\sum_{i=1}^4 3(1 + \cos^2\Theta_i)}{\sum_{i=1}^4 (5 - 3\cos^2\Theta_i)} = 1 \quad (2)$$

where the sum is taken over the four Fe with trigonal axes along the different  $\langle 111 \rangle$  directions. No angular dependence is expected and a single-crystalline sample has the same intensity ratio as a polycrystalline one, preventing the determination of the sign of  $V_{zz}$  from the angular dependence of the quadrupole components. Indeed we have measured a single-crystalline  $\epsilon$ -FeSi sample<sup>20</sup> and found that the ratio of the intensity of the two quadrupole components is, to within 1%, angular independent and equal to 1. In the following sections a different approach to the determination of the sign of  $V_{zz}$  and the asymmetry observed in polycrystalline  $\epsilon$ -FeSi samples will be presented and discussed.

#### A. Measurements in an external magnetic field

Due to an external magnetic field the degeneracy of the nuclear levels is completely removed. The EFG axes in a powder sample take all orientations with respect to the mag-

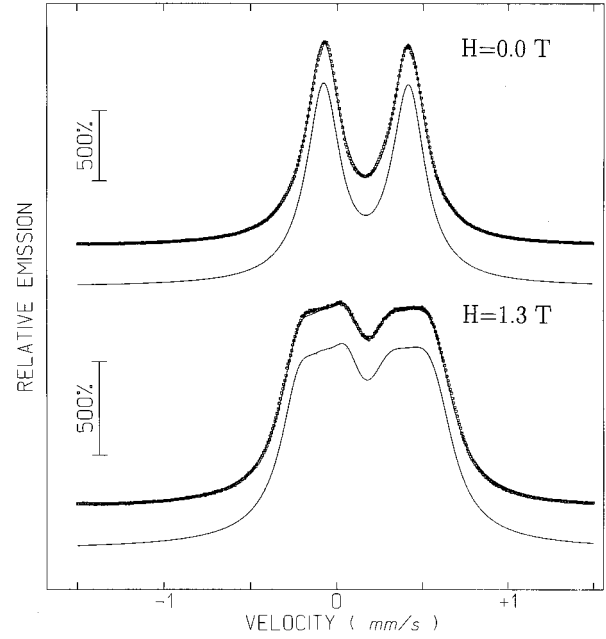


FIG. 2. CEM spectra of polycrystalline  $\epsilon$ -FeSi at  $H=0$  and  $H=1.3$  T with  $\theta=\pi/4$  and  $\alpha=\pi/2$ . The solid lines are the fits to the experimental data. For clarity they are also shown shifted.

netic field. For zero or small asymmetry parameter  $\eta$  the two-line zero-field spectrum splits, in a first-order perturbation treatment, into a doublet and a triplet<sup>21</sup> with the doublet due to the  $I_\pi$  transition. For  $^{57}\text{Fe}$  then if the doublet is at positive velocity (larger energy) the sign of  $V_{zz}$  is positive. Second-order perturbation effects, orientation of the crystallites, and anisotropic Debye-Waller factors can markedly alter the spectrum and prevent the determination of the sign of  $V_{zz}$ , particularly for small quadrupole splittings ( $<0.5$  mm/s).

The CEM spectrum, at  $H=0$ , of a 100 nm thick polycrystalline  $\epsilon$ -FeSi sample is shown in Fig. 2. The Mössbauer parameters, reported in Table I, are consistent with those previously reported for this phase.<sup>1,22,23</sup> The relatively narrow linewidth indicates also that deviations from the stoichiometric ratio 1:1 or the presence of other phases can be excluded. The interaction of the Fe nuclear quadrupole moment with an EFG, due to the  $C_3$  point symmetry, results in the observed quadrupole doublet. The asymmetry parameter  $\eta$  is zero due to the trigonal point symmetry.

Figure 2 shows the Mössbauer spectrum in an external magnetic field,  $H=1.3$  T, for the same sample. The angle between the direction of emission of the  $\gamma$  quantum and the surface normal,  $\theta$ , and between the direction of emission of the  $\gamma$  quantum and the external magnetic field  $H$ ,  $\alpha$ , were  $\theta=\pi/4$  and  $\alpha=\pi/2$ . The spectrum has been fitted using the

TABLE I. Mössbauer parameters for polycrystalline  $\epsilon$ -FeSi on Si(111) ( $\delta$  relative to  $\alpha$ -Fe at room temperature).

$H$ (T)	$H_{\text{fit}}$ (T)	$\delta$ (mm/s)	$\Gamma$ (mm/s)	$\Delta$ (mm/s)	$I_{>}/I_{<}$
0	-	0.282(5)	0.236(4)	0.495(4)	0.991(4)
1.3	1.20(5)	0.291(5)	0.260(5)	+0.502(5)	-

NORMOS-90 (Ref. 24) fitting program which allows the treatment of the magnetic perturbation based on the superoperator formalism<sup>25</sup> for a fixed angle  $\alpha$  and an isotropic distribution of the angles between the EFG principal axis and emission of the  $\gamma$  quantum directions. The quality of the fit and the consistency of the isomer shift and quadrupole splitting values with those obtained with  $H=0$  confirm that this condition is met, i.e., the absence of texture or significant stress in the investigated polycrystalline sample. The fitting parameters are reported in Table I. This analysis determines therefore that the sign of  $V_{zz}$  in  $\epsilon$ -FeSi is positive.

### B. Effect of internal stress

According to Eq. (1) for isotropic polycrystalline samples the ratio  $I_{>}/I_{<}$  is expected to be equal to 1, where  $I_{>}$  ( $I_{<}$ ) is the intensity of the higher (lower) energy transition. A small asymmetry  $I_{>}/I_{<} \neq 1$  of the order of 3–10 %, has been observed in polycrystalline thin films<sup>15</sup> depending on their preparation procedure (film thickness, annealing temperature, heating and cooling rate). Its angular dependence rules out an origin related to an anisotropy of the recoil-free fraction (Goldansky-Karyagin effect<sup>26</sup>) or to various relaxation mechanisms.<sup>27</sup> We propose that the asymmetry is related to internal stress in the samples due to changes of the average atomic volume during the silicide formation and to the difference in the linear thermal expansion coefficients of the substrate and the film.

The in-plane stress of  $\epsilon$ -FeSi layers calculated from the measured curvature<sup>28</sup> on samples produced on Si(111) [ $E/(1-\nu)=229$  GPa (Ref. 29)] was found to be tensile and equal to  $\sigma_{\parallel}=1.9(2)$  GPa. Using the elastic constants for  $\epsilon$ -FeSi,<sup>30</sup> one can calculate the strain parallel and perpendicular to the surface,  $\epsilon_{\parallel}=5.4 \times 10^{-3}$  and  $\epsilon_{\perp}=-3.2 \times 10^{-3}$ , respectively. Due to internal stress the four Fe atoms in the  $\epsilon$ -FeSi are not equivalent any more and those ( $\text{Fe}_1$ ) with the trigonal axis close to the surface normal are characterized by a reduction of the Fe-Si distance (compressive strain) while the other three ( $\text{Fe}_{2,3,4}$ ) have a larger Fe-Si distance (tensile strain). The EFG is therefore different at the two Fe sites and two different quadrupole doublets should characterize the Mössbauer spectrum resulting in the observed asymmetry. Indeed the CEM spectrum measured at  $\theta=0$  (see Fig. 3) shows two quadrupole doublets with parameters reported in Table II. The value  $I_{>}/I_{<}=2.4$  observed for  $\text{Fe}_1$  provides an independent confirmation that the sign of the value of the EFG component along the principal axes is positive. The reduction from the ideal value of 3.0 [see Eq. (1)] can be attributed to the distribution of  $\langle 111 \rangle$  directions around the surface normal and to a geometrical effect related to the finite size of the source and of the sample. The observed ratio for  $\text{Fe}_{2,3,4}$  is consistent with a random distribution of these trigonal axes, as expected for a polycrystalline sample. The ratio  $I_{>}/I_{<}=0.9$  for  $\text{Fe}_1$  with  $\theta=\pi/2$  (see Fig. 3), reported in Table II, is in good agreement with the value of 0.6 given by Eq. (1). The deviation is related to the previously discussed effects. The reduction of the point symmetry at the Fe sites resulting in the two angular dependent quadrupole doublets explains not only the observed asymmetry, but also its angular dependence. The CEM spectrum measured at  $\theta=\pi/2$  shows that the asymme-

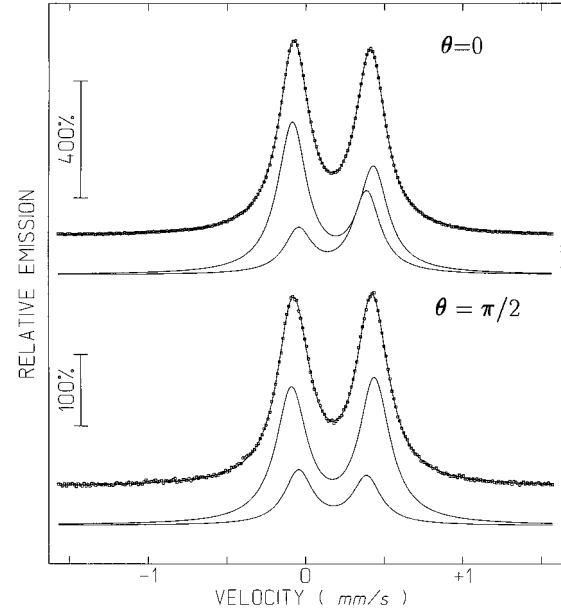


FIG. 3. CEM spectra of polycrystalline  $\epsilon$ -FeSi at  $H=0$  with  $\theta=0$  and  $\theta \approx \pi/2$ . The solid lines are the fits to the experimental data. The two quadrupole doublets used for the fit are shown shifted.

try is indeed angular dependent and that the intensity ratios of the quadrupole components is consistent with a strained polycrystalline  $\epsilon$ -FeSi.

## IV. THEORY

### A. Method of calculations

The electronic structure of  $\epsilon$ -FeSi was calculated with the full potential linear muffin-tin orbital (FPLMTO) method<sup>31</sup> using the local density approximation (LDA) for exchange and correlation effects.<sup>32</sup> This method expands the electron wave functions in terms of muffin-tin orbitals,<sup>33</sup> which are atom-centered Neumann functions augmented inside muffin-tin spheres by the numerical solution of the radial scalar-relativistic Dirac equation in the self-consistent crystal potential, together with the energy derivative of this solution.<sup>34</sup> This construction has proven very accurate for solid state calculations.<sup>35</sup> We used three different decay constants for the envelope functions. The basis set used included for each Fe atom 3 orbitals of  $s$  character,  $3 \times 3$  orbitals of  $p$  character,  $2 \times 5$  orbitals of  $d$  character, and  $1 \times 7$  orbitals of  $f$  character (in short, 3  $s$ , 3  $p$ , 2  $d$ , 1  $f$ ). Similarly, for the Si atoms basis functions were chosen as (3  $s$ , 3  $p$ , 2  $d$ ). No shape approximation for the crystal potential is invoked. The crystalline charge density is evaluated exactly within muffin-tin spheres, while in the interstitial region an interpolation scheme is used to obtain the charge density.<sup>31</sup> To further increase the accuracy of the interpolation scheme, additional “empty” muffin-tin spheres are included in the open regions of the unit cell [at positions  $(a, a - \frac{1}{2}, \frac{1}{2} - a)$ ,  $(\frac{1}{2} - a, a, a - \frac{1}{2})$ ,  $(a - \frac{1}{2}, \frac{1}{2} - a, a)$  and  $(-a, -a, -a)$ , with  $a = 1 - \frac{1}{2}(u_{\text{Fe}} + u_{\text{Si}})$ ]. For the evaluation of the Fe electric-field gradient it is important to include the Fe  $3p$  semicore states as band states, which has been done in a separate energy panel.

TABLE II. Mössbauer parameters for the polycrystalline  $\epsilon$ -FeSi on Si(111) on which the stress was measured ( $\delta$  relative to  $\alpha$ -Fe at room temperature).

Site	$\theta$	$\delta$ (mm/s)	$\Gamma$ (mm/s)	$\Delta$ (mm/s)	$I_{>}/I_{<}$	$A_i/\Sigma A_i$
Fe <sub>1</sub>	0	0.28(1)	0.21(1)	0.43(1)	2.4	0.26(2)
Fe <sub>2,3,4</sub>	0	0.28(1)	0.22(1)	0.51(1)	0.7	0.74(2)
Fe <sub>1</sub>	$\pi/2$	0.28(1)	0.22(1)	0.43(1)	0.9	0.25(2)
Fe <sub>2,3,4</sub>	$\pi/2$	0.28(1)	0.24(1)	0.53(1)	1.1	0.75(2)

The electric-field gradient tensor,  $\bar{V}$ , is calculated using the nonspherical part (in fact, the  $\ell=2$  component) of the crystalline Hartree potential, from which the second derivative tensor

$$V_{ij} = \frac{\partial^2 V_{H,\ell=2}}{\partial x_i \partial x_j}$$

is obtained. Denoting the eigenvalues of  $\bar{V}$  by  $V_{xx}$ ,  $V_{yy}$ , and  $V_{zz}$  with  $|V_{xx}| \leq |V_{yy}| \leq |V_{zz}|$ , the electric-field gradient per definition is equal to  $V_{zz}$ , while the asymmetry parameter is

$$\eta = \frac{V_{xx} - V_{yy}}{V_{zz}},$$

which lies in the range [0,1] (since  $V_{xx} + V_{yy} + V_{zz} = 0$ ). Due to the symmetry of the  $\epsilon$ -FeSi crystal structure, the direction of the field gradient is along the  $\langle 111 \rangle$  directions while the asymmetry parameter vanishes.

## B. Results

The electric-field gradient ( $V_{zz}$ ) at the Fe nucleus in  $\epsilon$ -FeSi is calculated to be  $+4.32 \times 10^{21}$  V/m<sup>2</sup>. The quadrupole splitting in velocity units for the  $\pm 3/2 \rightarrow \pm 1/2$  transition is

$$\Delta = \frac{eQV_{zz}c}{2E_0} \left( 1 + \frac{1}{3} \eta^2 \right)^{1/2}, \quad (3)$$

where  $E_0 = 14.41$  keV is the  $\gamma$ -ray energy, and  $Q$  is the nuclear quadrupole moment of the isomeric state of  $^{57}\text{Fe}$ . When the recent value<sup>11</sup> of  $Q = 0.16$  b is used one obtains a quadrupole splitting  $\Delta = +0.72$  mm/s. The positive sign is in accord with the experimental findings reported here, and the size is in excellent accord with the experimental  $T=0$  K value of  $\sim 0.74$  mm/s.<sup>1</sup> Additionally, the Fe electron contact density in  $\epsilon$ -FeSi is calculated to be lower than in  $\beta$ -FeSi<sub>2</sub> by  $1.01a_0^{-3}$ , and since the isomer shift of Fe in  $\beta$ -FeSi<sub>2</sub> is very close to that of  $\alpha$ -Fe,<sup>18,19</sup> we infer a theoretical isomer shift of  $\epsilon$ -FeSi relative to  $\alpha$ -Fe of  $\sim +0.22$  mm/s, using the calibration of Ref. 36. This is in reasonable agreement with the present experimental value of  $\delta \sim +0.28$  mm/s.

Other aspects of the electronic structure of  $\epsilon$ -FeSi have been studied. By minimizing the total energy as a function of volume, a theoretical lattice constant of  $a = 0.4377$  nm is obtained, which is 2.6% lower than the experimental value. While the LDA generally is known to underestimate lattice parameters, this deviation is still rather large and may indicate the presence of significant correlation effects in  $\epsilon$ -FeSi, which are not properly described with the LDA. On

the other hand, the optimized internal parameters,  $u_{\text{Fe}}$  and  $u_{\text{Si}}$ , are very close to the experimental values (within 1%), and not particularly sensitive to the volume. The electric field gradient is sensitive to both volume and internal parameters. The dependence on the structural parameters  $u_{\text{Fe}}$  and  $u_{\text{Si}}$  is shown in Fig. 4. In Fig. 4(a) the  $u_{\text{Si}}$  parameter is fixed at the theoretical optimal value  $u_{\text{Si}} = 0.844$ , while the  $u_{\text{Fe}}$  is varied and in Fig. 4(b) the  $u_{\text{Fe}}$  is fixed at  $u_{\text{Fe}} = 0.1358$ , while  $u_{\text{Si}}$  is varied. These results show that the quadrupole splitting is particularly sensitive to the  $u_{\text{Si}}$  parameter. Therefore, one might suggest that the unusual strong temperature dependence of the quadrupole splitting observed in  $\epsilon$ -FeSi is a consequence of the Si positions shifting with temperature. However, such a model seems inadequate in explaining the susceptibility anomaly and the specific heat anomaly of this compound. The values for the electric field gradient and isomer shift quoted above are all determined at the experimental structure.

Jaccarino *et al.*<sup>2</sup> explained the unusual behavior of  $\epsilon$ -FeSi with temperature in terms of a simple model with two

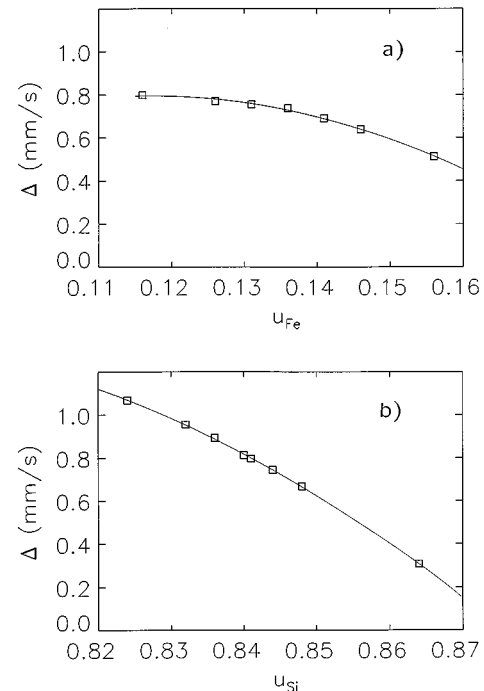


FIG. 4. Calculated dependence of the quadrupole splitting at the Fe nucleus as function of the structural parameters  $u_{\text{Fe}}$  and  $u_{\text{Si}}$ . (a)  $u_{\text{Si}} = 0.844$  is fixed. (b)  $u_{\text{Fe}} = 0.1358$  is fixed. The full lines are least-squares fits of the data points.

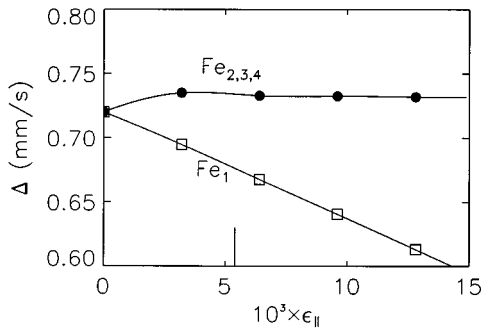


FIG. 5. Calculated quadrupole splitting as a function of  $\epsilon_{\parallel}$ . The ratio between  $\epsilon_{\parallel}$  and  $\epsilon_{\perp}$  is kept fixed at the experimentally determined value of  $-1.7$  (Ref. 30).  $\text{Fe}_1$  denotes the Fe atom at position  $u_{\text{Fe}}(1,1,1)$ , while  $\text{Fe}_{2,3,4}$  denotes the other three equivalent Fe atoms in the unit cell. The arrow indicates the value of the experimentally determined strain.

narrow bands on either side of a small  $\sim 0.1$  eV gap. The present LDA calculations, similar to others,<sup>37</sup> do find a narrow gap of size 0.10 eV (indirect, the lowest direct transition is at 0.15 eV). The density of states does exhibit small narrow peaks on both sides of the energy gap, but with a weight approximately a factor of 10 too low to explain the temperature dependences of the susceptibility and specific heat. We conclude, that a significant renormalization of the LDA bands must take place, as indeed suggested in the Kondo insulator model.<sup>4</sup>

In order to test the experimental conclusions regarding the influence of stress in the film, we have computed the electric-field gradient in a stressed geometry. Since the experimental strain field, as described, is given by the parameters  $\epsilon_{\parallel} = 5.4 \times 10^{-3}$  and  $\epsilon_{\perp} = -3.2 \times 10^{-3}$ , calculations were performed with values of the strain in a range which includes the experimental results, see Fig. 5. The calculations corroborate the experimental finding that the group of four Fe atoms of the unit cell splits into three equivalent atoms

( $\text{Fe}_{2,3,4}$ ) with a field gradient only slightly larger than the unstrained case (0.73 mm/s) and a single atom ( $\text{Fe}_1$ ) with a reduced field gradient (0.68 mm/s). At larger strains only the latter component shifts linearly with the strain. Thus, these calculations do confirm the experimental conclusion that the strain in the film causes a reduction in the quadrupole splitting of one of the Fe atoms. The observed relative changes of the quadrupole splittings of  $\text{Fe}_1$  and  $\text{Fe}_{2,3,4}$  are about 2–3 times larger than calculated, a fact which may be attributed to the general uncertainty, both in the determination of the experimental strain and in the theoretical work. In the latter, one should in principle minimize the total energy with respect to now four internal coordinates, which was not done here. Given the aforementioned strong dependency of the field gradient on the Si positions in the unit cell, this may lead to a non-negligible error in magnitude.

## V. CONCLUSIONS

The sign of the electric field gradient of  $\epsilon$ -FeSi has been determined to be positive by conversion electron Mössbauer spectroscopy in an external magnetic field and, independently, by the strain induced asymmetry of the intensity of the quadrupole components. These findings were corroborated by theoretical calculations with the *ab initio* full-potential LMTO method in the local density approximation. In view of the correlated nature of the  $\epsilon$ -FeSi compound it is astonishing that the electric-field gradient, being a rather sensitive quantity, may be computed with such good precision in this approach.

## ACKNOWLEDGMENTS

It is a pleasure to thank Professor J. R. Byberg for the use of the Varian EPR magnet. Two of us (M.F. and A.Z.) would like to thank Professor J. Böttiger for useful discussions. This work was supported by the Danish Accelerator Physics Council, the Natural Science Research Council, and NATO.

\*Permanent address: Moscow Engineering Physics Institute, 115 409 Moscow, Russia.

†Permanent address: Faculty of Applied Physics, Twente University, P.O. Box 217, 7500 AE Enschede, The Netherlands.

<sup>1</sup>G.K. Wertheim, V. Jaccarino, J.H. Wernick, J.A. Seitchik, H.J. Williams, and R.C. Sherwood, *Phys. Lett.* **18**, 89 (1965).

<sup>2</sup>V. Jaccarino, G.K. Wertheim, J.H. Wernick, L.R. Walker, and S. Arajis, *Phys. Rev.* **160**, 476 (1967).

<sup>3</sup>T.E. Mason, G. Aepli, A.P. Ramirez, K.N. Clausen, C. Broholm, N. Stücheli, E. Brucher, and T.T.M. Palstra, *Phys. Rev. Lett.* **69**, 490 (1992).

<sup>4</sup>D. Mandrus, J.L. Sarrao, A. Migliori, J.D. Thompson, and Z. Fisk, *Phys. Rev. B* **51**, 4763 (1995).

<sup>5</sup>L. Pauling and A.M. Soldate, *Acta Crystallogr.* **1**, 212 (1948).

<sup>6</sup>H. Watanabe, H. Yamamoto, and K. Ito, *J. Phys. Soc. Jpn.* **18**, 995 (1963).

<sup>7</sup>Y. Takahashi and T. Moriya, *J. Phys. Soc. Jpn.* **46**, 1451 (1979).

<sup>8</sup>S.N. Evangelou and D.M. Edwards, *J. Phys. C* **16**, 2121 (1983).

<sup>9</sup>K. Tajima, Y. Endoh, J.E. Fischer, and G. Shirane, *Phys. Rev. B* **38**, 6954 (1988).

<sup>10</sup>V.I. Anisimov, S.Yu. Exhov, I.S. Elfimov, I.V. Solovyev, and T.M. Rice, *Phys. Rev. Lett.* **76**, 1735 (1996).

<sup>11</sup>P. Dufek, P. Blaha, and K. Schwarz, *Phys. Rev. Lett.* **75**, 3545 (1995).

<sup>12</sup>N.E. Christensen, A. Svane, M. Fanciulli, G. Weyer, M. Methfessel, and C.O. Rodriguez, *Bull. Am. Phys. Soc.* **41**, 788 (1996).

<sup>13</sup>S.L. Ruby and P.A. Flinn, *Rev. Mod. Phys.* **36**, 351 (1964).

<sup>14</sup>S.S. Lau, J.S.-Y. Feng, J.O. Olowolafe, and M.-A. Nicolet, *Thin Solid Films* **25**, 415 (1975).

<sup>15</sup>M. Fanciulli, C. Rosenblad, G. Weyer, H. von Känel, N. Onda, V. Nevolin, and A. Zenkevich, in *Silicide Thin Films—Fabrication, Properties and Applications*, edited by R. T. Tung, K. Maex, P. W. Pellegrini, and L. H. Allen, MRS Symposia Proceedings No. 402 (Materials Research Society, Pittsburgh 1996), p. 319.

<sup>16</sup>G. Weyer, *Mössbauer Eff. Method.* **10**, 301 (1976).

<sup>17</sup>V.I. Goldanskii and R.H. Herber, *Chemical Applications of Mössbauer Spectroscopy* (Academic, London, 1968).

<sup>18</sup>M. Fanciulli, C. Rosenblad, G. Weyer, A. Svane, N.E. Christensen, and H. von Känel, *Phys. Rev. Lett.* **75**, 1642 (1995).

<sup>19</sup>M. Fanciulli, C. Rosenblad, G. Weyer, A. Svane, N.E. Chris-

- tensen, C.O. Rodriguez, and H. von Känel (unpublished).
- <sup>20</sup>CEMS has been performed on a  $\epsilon$ -FeSi single crystal (see Ref. 9) kindly provided by Y. Endoh and M. Onodera at Tohoku University, Japan.
- <sup>21</sup>R.L. Collins, *J. Chem. Phys.* **42**, 1072 (1965).
- <sup>22</sup>K. Vojtechovský and T. Zemčík, *Czech. J. Phys. B* **24**, 171 (1974).
- <sup>23</sup>Ö. Helgason and T.I. Sigfússon, *Hyperfine Interact.* **45**, 415 (1989).
- <sup>24</sup>R.A. Brand, *NORMOS-90* Mössbauer Fitting Program Package, Wissenschaftliche Elektronik GmbH, Starnberg, Germany.
- <sup>25</sup>N. Blaes, H. Fischer, and U. Gonser, *Nucl. Instrum. Methods B* **9**, 201 (1985).
- <sup>26</sup>V.I. Goldanskii, E.F. Makarov, and V.V. Khrapov, *Phys. Lett.* **3**, 344 (1963).
- <sup>27</sup>M. Blume, *Phys. Rev. Lett.* **14**, 96 (1965).
- <sup>28</sup>G.G. Stoney, *Proc. R. Soc. London* **A82**, 172 (1909).
- <sup>29</sup>W.A. Brantley, *J. Appl. Phys.* **44**, 534 (1973).
- <sup>30</sup>J.L. Sarrao, D. Mandrus, A. Migliori, Z. Fisk, and E. Bucher, *Physica B* **199 & 200**, 478 (1994).
- <sup>31</sup>M. Methfessel, *Phys. Rev. B* **38**, 1537 (1988); M. Methfessel, C.O. Rodriguez, and O.K. Andersen, *ibid.* **40**, 2009 (1989).
- <sup>32</sup>R.O. Jones and O. Gunnarsson, *Rev. Mod. Phys.* **61**, 689 (1989).
- <sup>33</sup>O.K. Andersen, *Phys. Rev. B* **12**, 3060 (1975).
- <sup>34</sup>See, e.g., H.L. Skriver, *The LMTO Method* (Springer-Verlag, Berlin, 1984).
- <sup>35</sup>O.K. Andersen, O. Jepsen, and O. Glötzel, in *Canonical Description of the Band Structures of Metals*, Proceedings of the International School of Physics, Course LXXXIX, Varenna, 1985, edited by F. Bassani, F. Fumi, and M.P. Tosi (North-Holland, Amsterdam, 1985), p. 59.
- <sup>36</sup>O. Eriksson and A. Svane, *J. Phys. Condens. Matter* **1**, 1589 (1989).
- <sup>37</sup>L.F. Mattheiss and D.R. Hamann, *Phys. Rev. B* **47**, 13 114 (1993).